Serrodyne Frequency Translation of Continuous Optical Signals Using Ultrawide-band Electrical Sawtooth Waveforms

Ilya Y. Poberezhskiy, *Member, IEEE*, Bartosz Bortnik, *Student Member, IEEE*, Jason Chou, Bahram Jalali, *Fellow, IEEE*, and Harold R. Fetterman, *Fellow, IEEE*

***Abstract*—Serrodyne frequency translation of continuous optical signals by $\pm$1.28 GHz is reported, significantly exceeding the highest previously published serrodyne shifts. To achieve these shifts, an ultrawide-band high-power electrical sawtooth created by spectral modulation of dispersed optical pulses was used. Its amplification involved a novel predistortion technique to compensate for the gain and phase ripple in the amplifier bandwidth.**

***Index Terms*—Electrooptic modulation, optical frequency conversion, optical pulse shaping, phase modulation, signal synthesis.**

I. Introduction

PHASE modulation of light with an electrical sawtooth of an appropriate amplitude results in an optical frequency shift that is inversely proportional to the sawtooth period. This type of phase modulation, described in detail below, is called serrodyne frequency translation and has been demonstrated in $LiNbO_3$ modulators by up to several megahertz [1]–[3]. It can be used in fiber optic gyroscopes [3], lidar velocimeters [4], spectroscopy, optical communications, shearing interferometry, and other applications.

The main factor limiting the maximum achievable serrodyne frequency shift has been the difficulty of generating and amplifying a high-speed sawtooth, due to its broad spectrum containing many harmonic components of the fundamental frequency. In this paper, we report using an RF-photonic arbitrary waveform generator (PAWG) based on the design described in [5] that has been substantially modified to produce a continuous high-power electrical sawtooth waveform. This sawtooth was then used to perform serrodyne frequency translation of a continuous-wave (CW) optical signal by 1.28 GHz, which exceeds the highest previously reported optical serrodyne frequency shift by almost two orders of magnitude.

Serrodyne frequency shifting is conceptually based on modulation of optical phase with a linear waveform $g(t) = at$ in an electrooptic (EO) modulator. As a result, the frequency of the modulated optical signal is shifted by the amount proportional to the slope a of the modulating waveform

$$\bar{E}(t,z) = \bar{E}_0 \exp[j(\omega t - kz + g(t))] = \bar{E}_0 \exp[j((\omega + a)t - kz)]. \quad (1)$$

Here, E is the electrical field of a monochromatic optical signal, E_0 is its amplitude, ω is the initial angular frequency, k is the wavevector, and z is the direction of propagation.

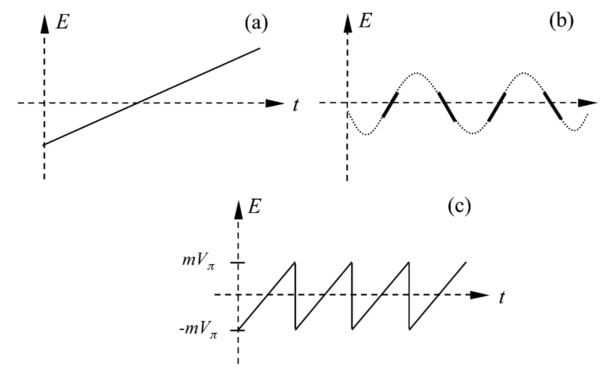

Fig. 1. Electric field temporal profiles that can be used for electrooptic frequency shifting. (a) Linear electric field. (b) Linear parts of a sinusoid. (c) Sawtooth with amplitude 2 mV_π.

Of course, an infinitely long linear signal [Fig. 1(a)] is not physically realizable, so an alternative waveform must be used for frequency shifting. A simple approach that allows shifting optical pulses by hundreds of GHz is phase modulation with linear regions of a sinusoid [Fig. 1(b)] that has been demonstrated in high-speed polymer [6], [7] and $LiNbO_3$ modulators [8]. However, it is limited to frequency translation of short optical pulses. As the frequency of the sinusoid increases, its linear portion has a greater slope yet shorter duration, therefore, this approach requires a tradeoff between the magnitude of the shift and the duration of the optical pulses that can be shifted.

In contrast, phase modulation with an electrical sawtooth can produce frequency translation of either CW or pulsed optical signals. To ensure phase continuity, the peak-to-peak amplitude of the modulating sawtooth must be an integer multiple of $2V_\pi$ [Fig. 1(c)]. Phase modulation with a sawtooth with fundamental frequency $f_{\rm st}$ (period $T_{\rm st} = 1/f_{\rm st}$) and peak-to-peak amplitude 2 mV_π, where m is a positive integer, produces a frequency shift of $mf_{\rm st}$. An upshift or a downshift is achieved depending on the slope of the ramped portion of the sawtooth.

Manuscript received July 19, 2005. This work was supported in part by the U.S. Air Force Office of Scientific Research.

I. Y. Poberezhskiy was with the Electrical Engineering Department, University of California, Los Angeles, CA 90095 USA. He is now with Caltech Jet Propulsion Laboratory, Pasadena, CA 91109 USA (e-mail: ilya@jpl.nasa.gov).

B. Bortnik, J. Chou, B. Jalali, and H. R. Fetterman are with the Electrical Engineering Department, University of California, Los Angeles, CA 90095 USA.

Digital Object Identifier 10.1109/JQE.2005.858467

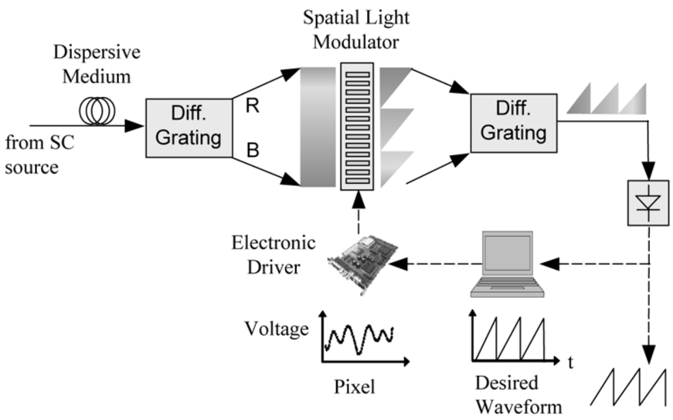

Fig. 2. Conceptual diagram of the RF photonic AWG. Note that the voltage applied to the SLM differs from the desired waveform to compensate for the system distortions.

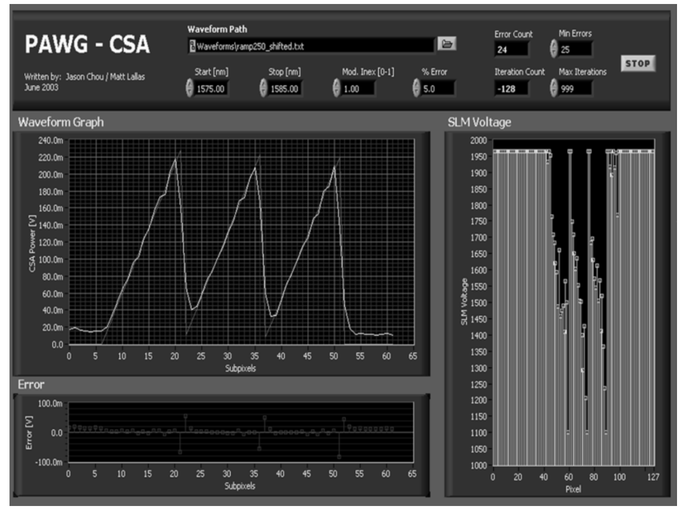

Fig. 3. PAWG LabVIEW user interface showing (top left) the desired and actual waveforms, (bottom left) the difference between them for each SLM pixel, and (right) the voltage applied to each SLM pixel.

Compared to acoustooptic (AO) frequency shifting, serrodyne frequency translation can potentially achieve larger frequency shifts with greater conversion efficiency, and does not require critical crystal alignment.

An alternative method of RF-photonic sawtooth generation, that employs reflections of optical pulses from multiple fiber Bragg gratings, and its use for serrodyne frequency translation was recently described in [9]. However, that technique does not enjoy the flexibility of the method presented below, and the demonstrated sawtooth has a frequency of 20 MHz, much lower than 1.28 GHz reported here.

This paper has the following structure. Section II describes the generation of a high-power continuous electrical sawtooth, covering the basic operation of our PAWG, production of continuous waveforms using repetition rate multiplication, and broad-band amplification of the sawtooth using a software-based predistortion technique. Section III describes the setup and results of the serrodyne frequency shifting experiment. Section IV discusses the obtained results and suggests some possible future improvements. Finally, Section V concludes the paper.

II. Generation of High-Power Ultrawideband Electrical Sawtooth

A. Optical Pulse Shaping Using Spectral Modulation and Dispersion

A PAWG conceptually similar to the one reported in [5] was used to create an RF pulse train with each pulse consisting of several periods of a sawtooth. The technique is schematically illustrated in Fig. 2. A passively mode-locked fiber laser with a 20-MHz repetition rate emits a train of ~200-fs pulses that are then spectrally broadened to over 100 nm in a supercontinuum (SC) fiber, where a combination of nonlinear optical effects such as self- and cross-phase modulation, four-wave mixing, and Raman scattering is utilized. The spectrally broadened pulses are temporally dispersed in a 5.46-km spool of single-mode fiber (SMF-28).

The pulses are then spatially dispersed with a diffraction grating before entering a one-dimensional array of 128 liquid crystal spatial light modulators (SLMs). The spatial aperture of the device was designed to modulate the portion of the L-band between 1570 and 1590 nm. Transmission through each SLM is individually controlled by the voltage applied to that pixel. As a result of the wavelength-to-pixel mapping, the optical spectrum is modulated with the applied waveform. The light is then focused back into a fiber by the second diffraction grating. Since the dispersive fiber produced a wavelength-to-time mapping, the spectral modulation at the SLM is transformed into temporal modulation. The modulated pulses are then detected with a fast photodiode (New Focus 1011) and amplified to produce the desired RF waveform. It is appropriate to note that the dispersive delay line (in this case, a spool of SMF-28) may follow the SLM instead of preceding it with no change in the outcome. In our experiment, we placed the dispersion first in order to reduce the peak power and avoid nonlinear effects.

As shown in Fig. 2 and later in Fig. 7, the PAWG employs feedback by splitting a portion of its output and sending it to a photodetector followed by a digital oscilloscope. A computer running specially-written LabVIEW software (Fig. 3) captures the waveform displayed on the scope and compares it to the desired output. It then runs an optimization routine that adjusts the voltage applied to each SLM pixel to minimize the error in that part of the optical spectrum.

The electrical output showing three periods of a sawtooth is shown in Fig. 4(b). It can be seen that the period of the sawtooth is 260 ps with a fast 30-ps reset time. The ultimate electrical bandwidth of the system is limited by the number of actively used SLM pixels (usually no more than 100) and the precision with which the pixels are matched to the optical spectrum. The spectrum-to-pixel matching is not perfect, particularly near the edges of the array; i.e., light with the same wavelength may be focused into several pixels. Typically, this limits the electrical bandwidth more than the response of the photodetector and amplifier, unless a high-power amplifier is used, as discussed in Section II-C. In practice, no more than about five sawtooth periods can be created with the required fast reset time and smooth linear ramp using 100 SLM pixels.

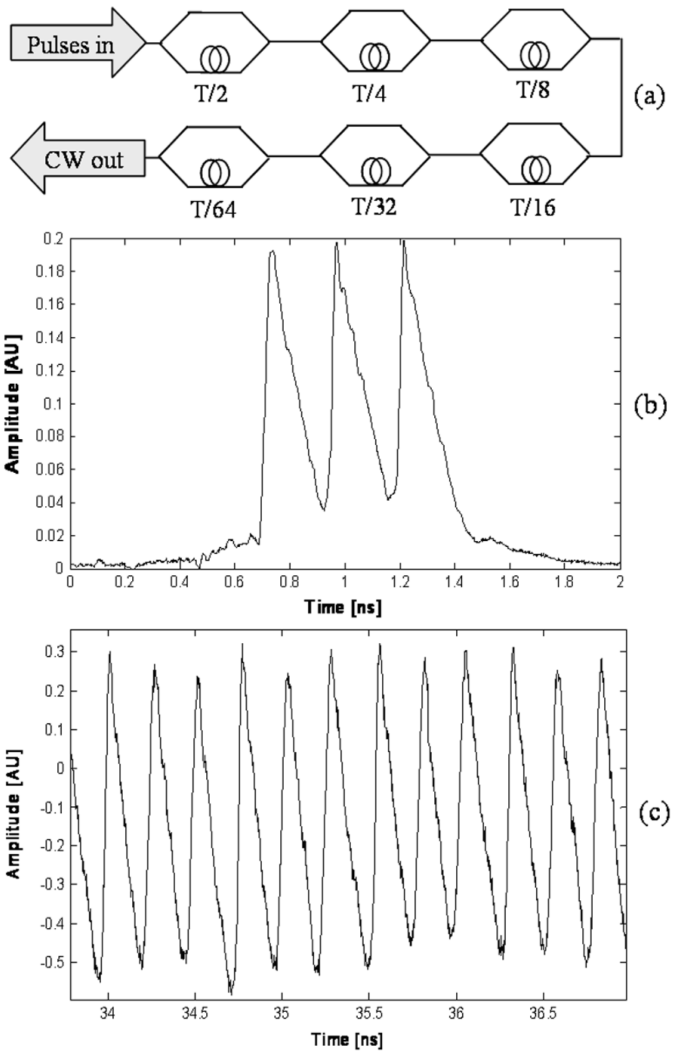

Fig. 4. Creation of a continuous waveform from modulated pulses. (a) Six-stage pulse repetition rate multiplier. (b) Three sawtooth periods produced by the PAWG. (c) Continuous 3.84-GHz sawtooth after the repetition rate multiplier.

B. Generation of Continuous Electrical Waveform

The PAWG reported in [5] and briefly described in Section II-A has an output that consists of a train of electrical pulses with the desired shape. However, a continuous electrical sawtooth is required to perform serrodyne frequency shifting. In order to create a continuous periodic waveform at the output, the modulated pulses need to be seamlessly merged together [10]. In other words, the duration of each modulated optical pulse before the photodetector must be equal to the period of the optical pulse train.

The mode-locked laser we used had the pulse repetition rate of 20 MHz, corresponding to a period of 50 ns. To create the sawtooth fragments shown in Fig. 4(b), we ultimately ended up using the part of the optical spectrum with the bandwidth of ~8.4 nm, as setting the transmission of the pixels near the edges of the SLM array to zero performs optical bandpass filtering. Approximately 350 km of SMF-28 would be required to stretch these optical pulses to 50 ns, which would not only be impractical, but would also create a sawtooth with a very long period.

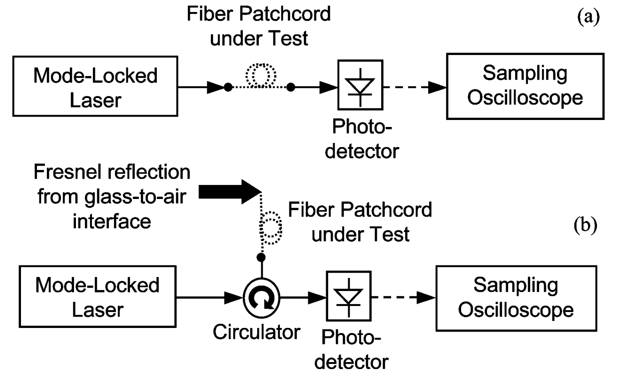

Fig. 5. Setup for accurately measuring group delay in a fiber patchcord connectorized on (a) both sides and (b) one side.

Therefore, we decided to make an inexpensive passive pulse repetition rate multiplier. It was comprised of a series of in-fiber variable delay stages, each one splitting the optical signal into 2 paths and introducing the path difference of $T/2^n$ in the nth stage [Fig. 4(a)]. Thus, each stage doubled the pulse repetition rate, and after passing through k stages, the repetition rate was multiplied by 2^k. We used six stages and as a result multiplied the repetition rate by 64 to obtain 1.28 GHz, corresponding to a period of 781 ps.

The delay lines in Fig. 4(a) were made using five 2×2 and two 1×2 fiber couplers. The path length difference was acheived by inserting carefully spliced fiber patchcords of the right lengths. To accurately measure these lengths before splicing, the position of a pulse on an oscilloscope was noted before and after inserting the fiber under test. When that fiber was connectorized on both sides, it was simply added in the transmission configuration [Fig. 5(a)]. When it was connectorized only on one side, it was attached to port 2 of a circulator in the reflection configuration [Fig. 5(b)] and a fraction of light was reflected from the fiber-air interface. The temporal displacement of the observed pulse after the fiber was inserted was equal to either the group delay in the fiber under test [Fig. 5(a)], or twice that group delay [Fig. 5(b)]. This technique allowed us to measure the delays with an accuracy of ~5 ps.

Another issue that proved particularly challenging was making sure that the light experienced equal loss in the two arms of each delay stage. The unavoidable difference in the splicing and connector losses between the two arms caused each set of pulses to have different amplitudes after passing through the repetition rate multiplier. This led to significant fluctuations in the amplitude of the output sawtooth. Even insubstantial differences in each stage could compound to produce noticeable amplitude fluctuations after all six stages. To the first order, the losses were matched by ensuring that the number of connectors in the two arms was the same. In addition, variable mechanical pressure controlled by a screw was applied to the fiber in the arm with the smaller loss to match the attenuation in the other arm. Less than 5% loss variation in each delay stage was achieved, allowing us to obtain the CW sawtooth shown in Fig. 4(c) with amplitude fluctuations low enough to demonstrate serrodyne frequency shifting.

A more precise loss-matching is possible if the light in both arms of each stage is passed through a commercially available multi-channel variable optical attenuator.

Certain amplitude fluctuations in the output are inevitable due to a more fundamental reason: the output of the mode-locked laser contains some optical power in the time span between the pulses. Thus, when the repetition rate is multiplied, the pulses interfere with the light already present in their new time slots. If the intensity of this light is just 0.01% of the main pulse, the electric field is 1%, so the fluctuations resulting from their coherent interaction after several differential delay stages can be noticeable. Fortunately, our system did not encounter this fundamental limitation that depends on the quality of the laser mode-locking.

C. Sawtooth Amplification Using Predistortion

The amplification of the sawtooth proved to be a challenging task. Typically, the voltage required to produce a 360° phase shift in state-of-the-art high-speed EO modulators (polymer or $LiNbO_3$) is $2V_\pi \approx 10$ Volt. Since RF loss and refractive index are frequency dependent, V_π is frequency dependent as well, so it is different for each harmonic component comprising the sawtooth spectrum. Let us assume here that V_π variations are negligibly small within the bandwidth of interest. A high-speed photodetector, such as New Focus 1011, has responsivity ~0.4 A/W and begins to saturate when the input optical power exceeds 1 mW. Thus, with a standard 50-Ω load, the electrical waveform at the output of the photodetector has the peak-to-peak amplitude of ~20 mV, and has to be amplified by 54 dB to reach 10 V. To achieve this, a cascade of two broad-band amplifiers was required. Agilent 83020A with the specified bandwidth of 2–26.5 GHz and the output power of 30 dBm served as the power amplifier. However, for both amplifiers in the cascade, and particularly the power amplifier, the gain and group delay were a function of frequency. This produced spectral and, consequently, temporal distortions of the output waveform that could not be corrected with feedback alone.

To overcome the amplifier distortion, a software-based predistortion technique was employed. The impulse response of the photodetector and the amplifier cascade $h(t)$ was measured by a sending a short optical pulse into the system. The Fourier transform of this impulse response gave us the transfer function of the system $H(\omega)$. By dividing the spectrum of the desired waveform $D(\omega)$ by $H(\omega)$, we attained the predistorted spectrum $P(\omega)$. The temporal waveform $p(t)$ obtained by taking an inverse Fourier transform of $P(\omega)$, should turn into the desired temporal waveform $d(t)$ after passing through the system.

In practice, this approach has many subtle points, e.g., the low frequency cutoff of the high-power RF amplifier induces significant fluctuations in the predistorted temporal waveform $p(t)$ that the PAWG is unable to generate unless the predistortion algorithm is significantly modified. The details of the predistortion algorithm will be published elsewhere.

To test the predistortion technique and create a high-power high-frequency sawtooth necessary for serrodyne frequency shifting, we decided to modulate each optical pulse with just one ramp (one sawtooth period) shown in Fig. 6(a). The calculated predistorted waveform applied to the SLM is shown in Fig. 6(b). The predistorted waveform produced by the SLM is shown in Fig. 6(c). When this waveform passed through the photodetector and amplifiers, it became a ramp shown in Fig. 6(d). Fig. 6(e) shows the continuous sawtooth obtained after this ramp was passed through the repetition rate multiplier. The resulting sawtooth had fundamental frequency of 1.28 GHz equal to the new pulse repetition rate, and peak-to-peak amplitude of 10 V.

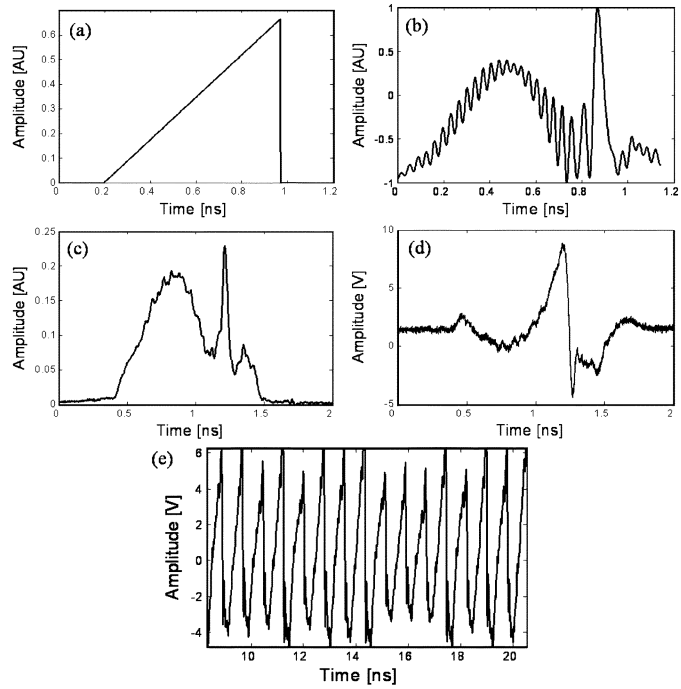

Fig. 6. High power sawtooth produced using the predistortion technique. (a) Desired sawtooth ramp. (b) Calculated predistorted ramp. (c) Predistorted ramp produced by SLM. (d) Amplified predistorted ramp. (e) Continuous sawtooth.

III. SERRODYNE EXPERIMENT

A. Setup

The block diagram of the serrodyne frequency shifting experiment [11] is shown in Fig. 7. The dotted box encloses the components used to generate and amplify the sawtooth. Continuous light from a Fitel laser diode was modulated in a Sumitomo $LiNbO_3$ phase modulator with 40 GHz optical bandwidth. We applied the sawtooth shown in Fig. 6(e) with a fundamental frequency $f_{st} = 1.28$ GHz and both positive and negative slope to observe an upshift and a downshift of the optical frequency. The sawtooth amplitude was tuned to maximize the suppression of the undesired sidelobes.

As in the previous experiments reported in [1]–[3] and [9], we indirectly detected optical serrodyne frequency shift by homodyning: mixing shifted and nonshifted light at a square-law photodetector and observing the mixing terms on an RF spectrum analyzer. However, unlike the previous experiments, we achieved a frequency shift sufficiently large to be directly resolved by a grating-based optical spectrum analyzer (OSA). For this purpose we used an Ando 6319 OSA with resolution bandwidth $\Delta\lambda = 10$ pm ($\Delta f = 1.25$ GHz at $\lambda = 1.55\ \mu$m).

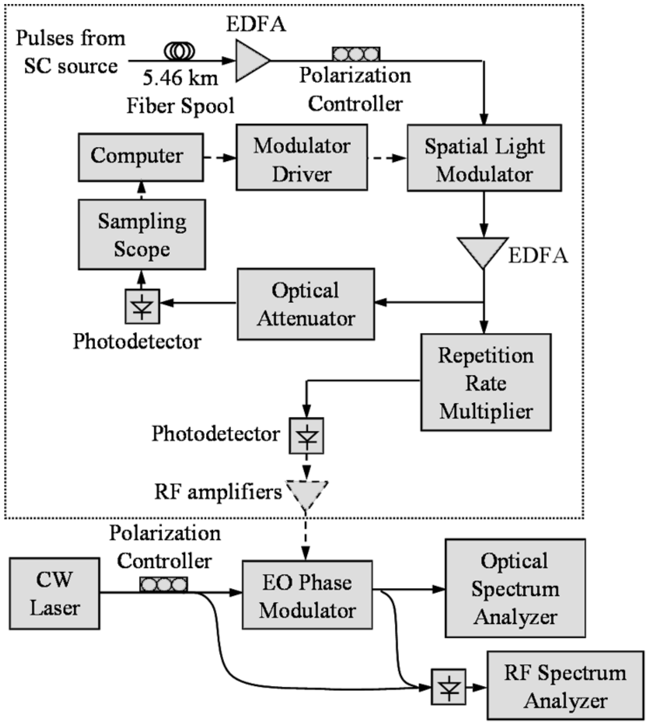

Fig. 7. Block diagram of the serrodyne frequency translator. Solid lines represent optical signals, dashed lines represent electrical signals, and the dotted line encloses the PAWG used to generate the sawtooth.

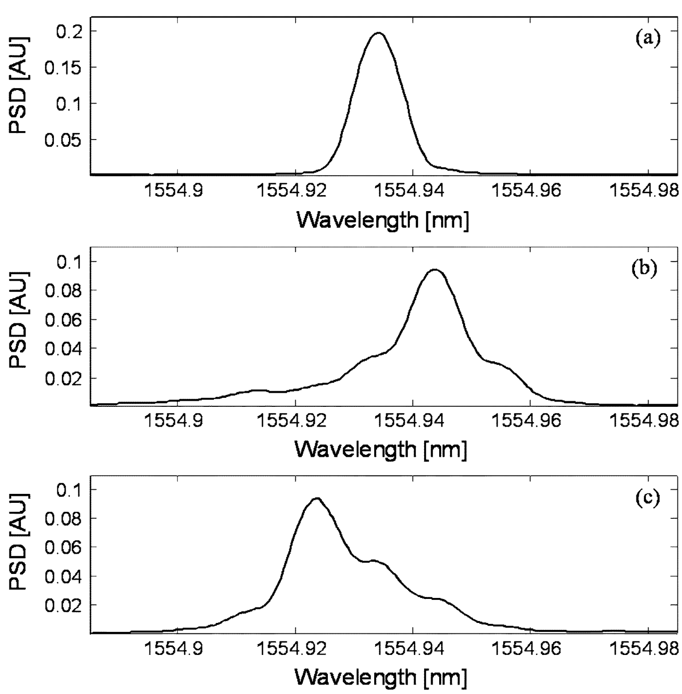

Fig. 8. Results of serrodyne frequency shifting observed on the OSA. (a) Initial, (b) downshifted, and (c) upshifted spectra are shown.

B. Results

The results of the frequency-shifting experiment are presented in Figs. 8 and 9. The initial spectrum is shown in Fig. 8(a), the downshifted (in frequency) spectrum is shown in Fig. 8(b), and the upshifted spectrum is shown in Fig. 8(c). The resolution of these plots is limited by the OSA resolution bandwidth which is much wider than the laser linewidth. As expected, both up and down shifts are equal to 1.28 GHz (10.24 pm). It can be seen that some energy of the shifted signal is present at undesired spectral components that do not appear discrete on the diagram because the OSA resolution Δf is just slightly smaller than the sawtooth frequency $f_{\rm st}$.

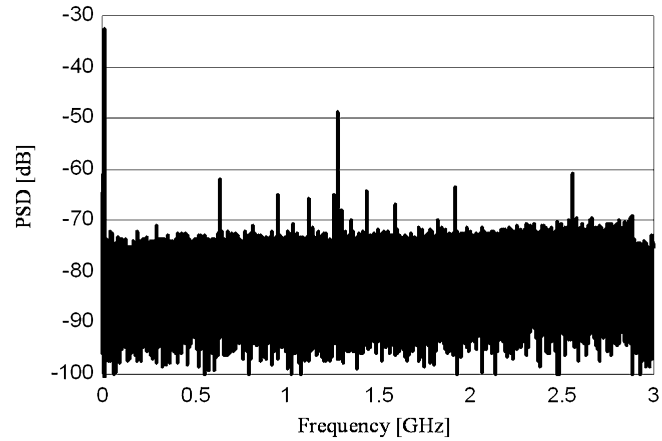

Fig. 9. Homodyne mixing spectral terms on the RF spectrum analyzer.

Fig. 9 shows the mixing terms observed on the RF spectrum analyzer. As expected the dominant term is at 1.28 GHz and corresponds to the serrodyne frequency shift that took place. The next highest mixing term is at 2 $f_{\rm st} = 2.56$ GHz and it is $\sim$12 dB below the first harmonic. The reasons for the presence of these undesired spectral components and the techniques for their improved suppression are discussed below.

IV. Discussion

The fact that after undergoing phase modulation with the sawtooth with fundamental frequency $f_{\rm st}$ and amplitude $2V_\pi$ most optical power is shifted from frequency f_0 to frequency $f_0 + f_{\rm st}$ or $f_0 - f_{\rm st}$ indicates that serrodyne frequency shifting has indeed taken place. At the same time, a portion of the optical signal remains at f_0 or is shifted to the undesired frequencies, particularly $f_0 \pm kf_{\rm st}$, where k is an integer. This is expected due to the imperfections of the modulating sawtooth such as amplitude fluctuations, finite reset time, and imperfect linearity of the ramped portion. Reference [3] establishes finite reset time as a particularly stringent constraint on the achievable undesired sidelobe suppression.

The imperfections mentioned above are noticeable in the sawtooth plotted in Fig. 6(e), which is not surprising since its parameters substantially advance the state of the art in ultrawide-band high-power waveform generation. However, the imperfections can be traced to two shortcomings of the described system that are not fundamental and leave significant room for future improvement.

The first is the inability of the SLM to reproduce high frequency oscillations in the calculated predistorted waveform shown in Fig. 6(b). An SLM array with a larger number of pixels would be able to reproduce these features, provided that the pixel-to-wavelength alignment was sufficiently accurate. The number of active pixels used in our experiment was the main bandwidth bottleneck, since the photodetector would have no trouble picking up these 27 GHz oscillations. A more accurate reproduction of the predistorted waveform before the power amplifier would enable a higher quality sawtooth after the amplifier, which in turn would significantly improve the undesired sidelobe suppression in the frequency shifted signal.

Another source of nonideal behavior mentioned in Section III-B is the difference in loss between the two arms of each repetition rate multiplier stage. Therefore, after passing through the repetition rate multiplier, the ramp amplitudes are uneven and cannot be equal to 2 V_π for all ramps. In the experiment, we tried to balance the losses in the two arms by applying pressure on fibers with screws. As a result, we were able to achieve transmission uniformity of about 5% between the two arms in each stage. However, after six stages the amplitude difference between the smallest and the largest ramps compounded to almost 30%. This difference could be substantially reduced if light in each arm of every stage passed through a multichannel computer-controlled variable attenuator.

To summarize, the quality of ultrawide-band high-power waveforms generated using the approach described in this paper can be undoubtedly improved in the future. These improvements will enable even larger gigahertz-range serrodyne frequency shifts with better suppression of undesired sidelobes. Such optical serrodyne frequency shifters should find numerous applications in many areas of optical technology.

V. Conclusion

Serrodyne frequency shifting of a continuous optical signal by more than one gigahertz has been demonstrated for the first time. To achieve it, we have generated a high-frequency, high-power electrical sawtooth waveform by employing an RF-photonic technique that uses spectral modulation of broad-band optical pulses in a spatial light modulator. A novel predistortion algorithm was used to compensate for the gain and phase ripple in the power amplifier's bandwidth.

Further improvements of the demonstrated approach will allow the generation of high-power sawtooth (and other periodic) waveforms with even higher fundamental frequencies and less distortion. This should enable optical serrodyne frequency shifters that are capable of producing larger frequency shifts with better suppression of unwanted sidelobes.

The reported serrodyne frequency shift exceeds the previously published results by almost two orders of magnitude. This dramatic extension of the range available to this technique should enhance its attractiveness for a variety of applications, such as coherent lidar, communications, spectroscopy, and optical gyroscopes.

References

[1] K. K. Wong, R. M. De La Rue, and S. Wright, "Electro-optic-waveguide frequency translator in $LiNbO_3$ fabricated by proton exchange," *Opt. Lett.*, vol. 7, pp. 546–548, 1982.

[2] L. M. Johnson and C. H. Cox, "Serrodyne optical frequency translation with high sideband suppression," *J. Lightw. Technol.*, vol. 6, no. 1, pp. 109–112, Jan. 1988.

[3] C. Laskoskie, H. Hung, T. El-Wailly, and C. L. Chang, "Ti-$LiNbO_3$ waveguide serrodyne modulator with ultrahigh sideband suppression for fiber optic gyroscopes," *J. Lightw. Technol.*, vol. 4, no. 1, pp. 600–606, Apr. 1989.

[4] D. Chang, G. Cardell, A. San Martin, and G. Spiers, "Coherent laser instrument would measure range and velocity," *NASA Tech Briefs*, vol. 29, pp. 28–30, 2005.

[5] J. Chou, Y. Han, and B. Jalali, "Adaptive RF-photonic arbitrary waveform generator," *IEEE Photon. Technol. Lett.*, vol. 15, no. 4, pp. 581–583, Apr. 2003.

[6] I. Y. Poberezhskiy, B. J. Bortnik, S.-K. Kim, and H. R. Fetterman, "Electrooptic polymer frequency shifter activated by input optical pulses," *Opt. Lett.*, vol. 28, pp. 1570–1572, 2003.

[7] H. R. Fetterman, S.-K. Kim, K. Geary, I. Poberezhskiy, B. Bortnik, W. Yuan, Y.-C. Hung, B.-J. Seo, and W. H. Steier, "Novel configurations and approaches for polymer electro-optic devices," *Pro. SPIE*, vol. 5351, no. 1, pp. 16–27, Jun. 2004.

[8] D. A. Farías and J. N. Eckstein, "Dynamic electrooptic frequency shifter for pulsed light signals," *IEEE J. Quantum Electron.*, vol. 41, no. 1, pp. 94–99, Jan. 2005.

[9] M. Shen and R. A. Minasian, "Serrodyne optical frequency translation using photonics-based waveforms," *Electron. Lett.*, vol. 40, pp. 1545–1547, 2004.

[10] J. Chou, I. Poberezhskiy, B. Bortnik, H. Fetterman, and B. Jalali, "Ultrawideband continuous sawtooth generation using RF-photonic technique," in *Proc. IEEE LTIMC 2004—Lightwave Technologies in Instrumentation and Measurement Conf.*, Oct. 2004, pp. 253–254.

[11] I. Poberezhskiy, B. Bortnik, J. Chou, B. Jalali, and H. Fetterman, "GHz-range serrodyne frequency shifting of continuous optical signals," in *Proc. 17th Annu. Meeting IEEE Laser Electo-Optics Society*, vol. 1, Nov. 2004, pp. 278–279.

Ilya Y. Poberezhskiy (S'01–M'04) received the B.S. (hons.), M.S., and Ph.D. degrees in electrical engineering from University of California, Los Angeles (UCLA), in 1999, 2001, and 2004, respectively.

Currently, he is with the Active Optical Sensing Group, Caltech Jet Propulsion Laboratory, Pasadena, CA. His research interests include optical frequency shifting, polymer electrooptic devices, and ultrafast arbitrary waveform generation. Recently, he has been working on interaction of light with large molecules and the metrology source subsystem for the upcoming NASA Space Interferometry Mission.

Bartosz Bortnik (S'01) received the B.S. degree in engineering physics in 2001 and the M.S. degree in electrical engineering in 2005 from the University of California, Los Angeles (UCLA), where he is currently working toward the Ph.D.

He is presently with the Millimeter Wave and Optoelectronics Laboratory, UCLA, working on high-speed rf-photonic systems. His research interests include ultrafast waveform generation and high-speed electrooptical systems.

Jason Chou was born in Walnut Creek, CA, on October 25, 1978. He received the B.S. (hons.) and M.S. degrees in electrical engineering from the University of California, Los Angeles (UCLA), in 2000 and 2002, respectively. He is currently working toward the Ph.D. degree at UCLA.

He conducts research in microwave photonics and nonlinear optics.

Bahram Jalali (S'86–M'89–SM'97–F'04) is currently a Professor of Electrical Engineering, the Director of the Defense Advanced Research Projects Agency (DARPA) Center for Optical A/D System Technology (COAST), and the Director of the Optoelectronic Circuits and System Laboratory, University of California at Los Angeles (UCLA). From 1988 to 1992, he was a Member of the Technical Staff with the Physics Research Division, AT&T Bell Laboratories, Murray Hill, NJ, where he conducted research on ultrafast electronics and opto-electronics. He was responsible for the successful development and delivery of 10-Gb/s lightwave circuits to the U.S. Air Force in 1992. From 1999 to 2001, while on leave from UCLA, he founded Cognet Microsystems, a Los Angeles-based fiber-optic component company that was acquired by the Intel Corporation in 2001. He currently serves as a consultant for the Wireless Networking Group (WNG) of the Intel Corporation and serves on the Board of Trustees of the California Science Center. He has authored or coauthored over 120 publications. He holds five U.S. patents. His current research interests are microwave photonics, integrated optics, and fiber-optic integrated circuits.

Dr. Jalali is a member of the California Nano Sciences Institute (CNSI) and is the chair of the Los Angeles Chapter of the IEEE Lasers and Electro-Optics Society (LEOS). He was the general chair for the 2001 IEEE International Conference on Microwave Photonics (MWP) and its Steering Committee chair (2001–present). He was the recipient of the BridgeGate 20 Award in recognition of his contributions to the Southern California hi-tech economy.

Harold R. Fetterman (SM'81–F'90) received the B.A. degree (hons.) in physics from Brandeis University, Waltham, MA, in 1962 and the Ph.D. in physics from Cornell University, Ithaca, NY, in 1968.

He joined Lincoln Laboratory in 1969, where his initial research concentrated on the use of submillimeter sources for spectroscopy. In 1982, he joined the Electrical Engineering Department of the University of California, Los Angeles (UCLA), as a Professor and served as the first Director of the Center for High Frequency Electronics. His research has concentrated on combining high-frequency structures and systems with optical devices. These efforts include continuous-wave optical mixing experiments using three terminal devices, high-speed polymer optical modulators, and traveling-wave photodetectors, which are now being extended to over 200 GHz. Some of these devices have been incorporated into novel systems such as optically controlled phased-array radars and, more recently, new forms of optical analog-to-digital converters.

Dr. Fetterman is a Fellow of the Optical Society of America (OSA).